

Copper crystals on the $(11\bar{2}0)$ sapphire plane: orientation relationships, triple line ridges and interface shape equilibrium

Stefano Curiotto · Harry Chien · Hila Meltzman ·
Stephane Labat · Paul Wynblatt · Gregory S. Rohrer ·
Wayne D. Kaplan · Dominique Chatain

Received: 18 September 2012 / Accepted: 7 December 2012 / Published online: 20 December 2012
© Springer Science+Business Media New York 2012

Abstract The orientation relationships (ORs) of copper crystals on a $(11\bar{2}0)$ sapphire substrate equilibrated at 1253 K are presented. They barely depend on the procedures used in sample preparation, i.e. dewetting of a copper film in the liquid state or in the solid state. The most frequent OR found is $\text{Cu}(111) \parallel \text{Al}_2\text{O}_3(11\bar{2}0)$ and $\text{Cu}[1\bar{1}0]$ within few degrees from $\text{Al}_2\text{O}_3[0001]$. A secondary, lower frequency OR is also observed: $\text{Cu}(001) \parallel \text{Al}_2\text{O}_3(11\bar{2}0)$ with $\text{Cu}[1\bar{1}0]$ within a few degrees from either $\text{Al}_2\text{O}_3[1\bar{1}00]$ or $\text{Al}_2\text{O}_3[0001]$. These ORs do not follow the Fecht and Gleiter model which proposes that dense directions of the metal should align with dense directions of the oxide. On annealing, even at a temperature about half of the melting point of sapphire, fast diffusion of sapphire at the copper/sapphire interface is observed: the copper particles tend to achieve their interfacial equilibrium shapes by sinking into the substrate, and sapphire ridges form at the triple line. Finally, it is shown that the $\text{Cu}(111) \parallel \text{Al}_2\text{O}_3(11\bar{2}0)$ interface remains flat at the atomic scale, and is therefore part of the copper/sapphire equilibrium interfacial shape.

Introduction

The interfacial energy of hetero-interfaces and its anisotropy in crystalline materials are fundamental thermodynamic properties of those interfaces. Many technologically important devices contain metal–ceramic interfaces which are difficult to study due to the complexity of their structure and crystallography. This paper addresses the preferred orientation relationships (ORs) of copper crystals equilibrated on a sapphire surface terminated by the $(11\bar{2}0)$ crystal plane (also referred to as the a-plane) and the morphology of that interface. The present study follows a previous investigation of the ORs of copper crystals on the (0001) plane (c-plane) of sapphire [1]. Our ultimate goal is to understand the key parameters that determine the OR of fcc metals on sapphire by studying the behavior of several different interfaces in the copper/sapphire system.

For a sapphire crystal terminated by a surface of given orientation, there may be several minima (cusps) in the orientation dependence of the energy of the copper/sapphire interfaces. Since the surface energy of pure copper is almost isotropic (its surface energy anisotropy is only about 1 % at 1240 K [2]), the preferred, minimum energy OR will correspond to the deepest minimum of the copper/sapphire interfacial energy. However, in a system consisting of a large number of metal crystals on a given single-crystal oxide surface, several ORs may be observed, even after long anneals, as shown by X-ray diffraction (XRD) [3], by electron backscatter diffraction (EBSD) [1], or by high resolution transmission electron microscopy (HRTEM) methods [4]. This indicates that certain metallic crystals are unable to rotate on the oxide surface in order to reach the lowest energy equilibrium OR, or that they may be trapped in local energy minima [5] under conditions

S. Curiotto (✉) · D. Chatain
Aix Marseille Université, CNRS, CINaM UMR 7325,
13288 Marseille, France
e-mail: curiotto@cinam.univ-mrs.fr

H. Chien · P. Wynblatt · G. S. Rohrer
Department of Materials Science and Engineering, Carnegie
Mellon University, Pittsburgh, PA 15213, USA

H. Meltzman · W. D. Kaplan
Department of Materials Science and Engineering,
Technion-Israel Institute of Technology, 32000 Haifa, Israel

S. Labat
Aix Marseille Université, CNRS, IM2NP UMR 6242,
13397 Marseille, France

where the activation barrier for rotation out of these minima is too high. HRTEM observations on different ORs performed by different authors [4, 6] for copper crystals on (0001) plane sapphire suggest that the observed ORs in that system are highly dependent on the procedures used in sample preparation, which determine the atomic binding at the interface. This issue has recently been pointed out by Curiotto et al. [1].

Investigations of the OR of fcc metals on the $(11\bar{2}0)$ surface (a-plane) of sapphire are scarce compared to those available for the c-plane. Scheu et al. [7] performed HRTEM studies of copper films deposited by physical vapor deposition (PVD) under ultra high vacuum (UHV) at 1073 K on the a-plane of sapphire in which they identified the following OR: $\text{Cu}(111)[1\bar{1}0] \parallel \text{Al}_2\text{O}_3(11\bar{2}0)[1\bar{1}00]$. Sasaki et al. [4] found a different OR when Cu films are prepared by pulsed laser deposition at 1073 K on the a-plane of sapphire: $\text{Cu}(001)[1\bar{1}0] \parallel \text{Al}_2\text{O}_3(11\bar{2}0)[0001]$, as well as a minor OR: $\text{Cu}(111)[1\bar{1}0] \parallel \text{Al}_2\text{O}_3(11\bar{2}0)[0001]$, which is rotated by 90° with respect to that found by Scheu et al. Vargas et al. [8] examined Ir and Pt films prepared on a-sapphire by metallo-organic chemical vapor deposition in the temperature range from 873 to 973 K. These fcc metals which have lattice parameters larger than that of Cu (by 6 % for Ir and 8 % for Pt) present different ORs: $\text{Ir}(100)[011] \parallel \text{Al}_2\text{O}_3(11\bar{2}0)[1\bar{1}00]$ and $\text{Pt}(111)[1\bar{1}0] \parallel \text{Al}_2\text{O}_3(11\bar{2}0)[1\bar{1}00]$. Later, Dai et al. [9] confirmed the OR of Ir deposited by PVD at 1073 K under UHV. However, thin metallic films on substrates are generally metastable, so that the ORs obtained using continuous thin films may be significantly influenced by the film surface energy rather than the film/substrate interfacial energy. Chatain et al. [2] studied copper crystals prepared by dewetting Cu films in the liquid state on sapphire(1120). They reported that the principal OR measured at 1240 K by X-ray diffraction is $\text{Cu}(111)[1\bar{1}0] \parallel \text{Al}_2\text{O}_3(11\bar{2}0)[0001]$. Although the (111) plane is parallel to the substrate in the case of Pt and Cu, it is the (001) plane that lies parallel to the a-plane in the case of Ir. However, in all these cases, one of the densely packed $\langle 110 \rangle$ directions on the metal side of the interface is aligned with either or both of the relatively densely packed [0001] and $[1\bar{1}00]$ directions of the sapphire substrate in agreement with the Fecht and Gleiter [3] lock-in model.

In addition to the ORs of copper crystals on the sapphire a-plane, the topographic nature of the sapphire surface after its equilibration with copper particles has also been investigated in the present study. When a particle partially wets a flat substrate, the forces perpendicular to the substrate that result from the various surface energies acting at the triple line are unbalanced (see for example [10] and the references therein). Under conditions where mass transport

is possible (as is the case in the present experiments), the shape of the particle–substrate system can evolve so as to eliminate the imbalance of interfacial forces, as has been described by Saiz et al. [11] and observed for copper crystals with small addition of titanium on c-sapphire at 1253 K [12]. In particular, substrate material from beneath the particle may be transported to ridges at the triple line that change the local shape so that an equilibrium dihedral angle is achieved. When interfaces are anisotropic, as in the case of sapphire–copper, the equilibrated 3D-shape of the particle–substrate system can be quite complex [13, 14]. In general, sapphire facets with orientations that are different from those of the original sapphire surface may develop at the copper–sapphire interface. Thus, it is quite possible for the presence of those new sapphire interfacial orientations to affect the observed ORs of the copper with respect to the substrate. These issues will also be addressed in this paper.

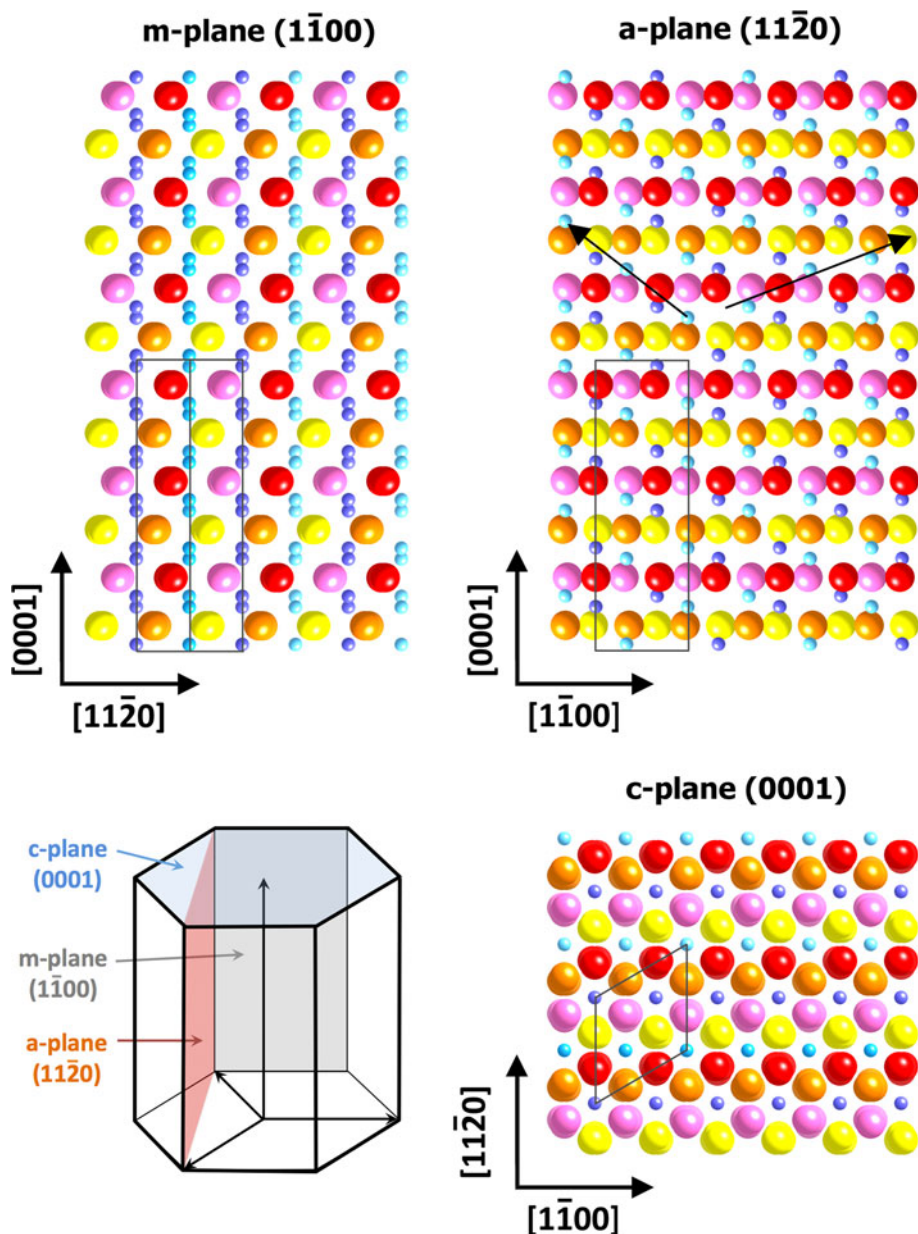
The $(11\bar{2}0)$ surface of sapphire

In order to understand possible alignments between copper and sapphire planes or directions, it is important to consider the ideal atomistic structure of the a-plane of sapphire. Figure 1 presents the crystallographic bulk arrangement of the Al and O ions in the a-plane of sapphire. In this figure, the oxygen ions (large spheres) and the aluminum ions (small spheres) have been colored differently depending on their distance from the a-surface along the $[11\bar{2}0]$ direction, which is perpendicular to the a-surface.

Along this direction, the ions are organized into stacks of one layer of Al ions (light blue or blue) and two layers of O ions (red and orange or pink and yellow). These ion planes can be easily seen in the c-plane and the m-plane, which are both perpendicular to the a-plane. A 3D unit cell is made of two of these stacks shifted in the two principal in-plane directions $[1\bar{1}00]$ and $[0001]$. If only O ions are considered, there is a mirror symmetry along the $[1\bar{1}00]$ direction. However, when the Al ions are taken into account, the a-plane no longer displays mirror symmetry. This is worth mentioning, as it affects the number of equivalent orientation relationships of copper crystals on the substrate.

There are two kinds of dense oxygen rows: the densest rows are made up of “almost” coplanar oxygen ions (red spheres), which lie parallel to the $[1\bar{1}00]$ direction and other rows that lie at $\pm 57.6^\circ$ to the $[1\bar{1}00]$ direction in which the oxygen ions (red and orange) alternatively belong to two adjacent planes.

Fig. 1 Crystallography of the a-plane of sapphire. At the *bottom left*, a sketch highlights the location of the a-plane, the m-plane, and the c-plane in a sapphire crystal. The other figures display the projection of the bulk atomic structure in each of these planes. The large spheres are oxygen ions (*red, orange, pink, and yellow* in order of increasing distance from the a-surface along the $[1\bar{1}\bar{2}0]$ direction). The small spheres are aluminum ions (*light blue and blue*, also in order of increasing distance). On each plane, the projection of the unit cell of sapphire is added. *Two arrows mark two dense directions of Al ions*, as explained in the text



The Al ions (light blue) of the surface plane are coplanar. The densest rows of Al, in which Al ions are paired, are parallel to the $[0001]$ direction. There are also dense rows at -51.7° from $[0001]$ in which Al ions are equidistant (arrow toward the upper left in Fig. 1). These rows occur in pairs. Finally, there are “wavy” Al rows at 68.5° from the $[0001]$ direction (arrow toward the upper right in Fig. 1).

Experimental procedures

Most of the procedures employed here have been described in a previous paper, in which the ORs of copper on

c-sapphire substrates [1] were reported. It is worth noting, for the purpose of subsequent comparisons, that samples in which the substrates were oriented along the a- and c-planes of sapphire were prepared simultaneously so as to ensure identical experimental conditions. Details regarding the a-plane samples are given in Table 1.

Copper films were deposited on sapphire($11\bar{2}0$) substrates and subsequently dewetted to form isolated copper crystals. The substrates consisted of single-side epipolished sapphire wafers, 5.08 cm in diameter, purchased from Gavish Industrial Technologies & Materials (Omer, Israel). These crystals have a maximum miscut of 0.1° and the following maximum impurity concentrations: Mg (20 ppm), Si (15 ppm), Na (10 ppm), Ca (7 ppm), and

Table 1 Parameters and characteristics of sample preparation

	TA20	TA22	TA25
Pre-treatment of sapphire prior to Cu deposit	1253 K for 78 h	1253 K for 78 h	1253 K for 200 h
Surface characterization of sapphire after pre-treatment (AES)	C (trace), Ca	C, Ca, Mo	C, Ca, Mo
Mode of Cu dewetting	Liquid-state	Liquid-state	Solid-state
Annealing time at 1253 K	20 h	6 h	78 h
Cu crystal size	$\approx 1 \mu\text{m}$	$\approx 500 \text{ nm}$	From a few nm to a few μm

K (0.5 ppm). After ultrasonic cleaning in ethanol for a few minutes, the surface chemistry of the wafers was investigated by Auger electron spectroscopy (AES) and found to consist of Al and O species with traces of C contamination.

The sapphire substrates were first annealed for several tens of hours at 1253 K in an Ar–20 %O₂ atmosphere in a furnace fitted with a sapphire tube as described in [15]. After annealing and cooling to room temperature, the sapphire surfaces were re-analyzed by AES to identify any species which may have segregated to the surface or that may have deposited on the surfaces from the environment during annealing. The three cleanest substrates were selected for investigation of copper ORs, and are subsequently referred to as TA20, TA22, and TA25. Table 1 summarizes the main features of these samples. Ca was detected at the surfaces of all the samples together with traces of Mo on TA22, TA25. Some C contamination was acquired during sample transfer through air. Taking into account the size of the Auger peaks and the coverage calculated for Ca [15], the total coverage of cation impurities is estimated to be less than 0.3 monolayers for all three samples.

The surface morphologies were investigated by atomic force microscopy (AFM) using a Park model XE-100 instrument [15]. Due to the small miscut, all substrate surfaces consisted of steps (230 pm in height) and terraces ($\sim 500 \text{ nm}$ in width).

After substrate preparation, copper films were deposited by PVD in a UHV chamber fitted with capabilities for AES analysis. The film surfaces were analyzed by AES, and traces of S and Cl were detected. These species were removed during the subsequent annealing of the film under Ar–H₂ [2]. The film thickness ranged from 30 to 100 nm, as measured by AFM.

The last stage of preparation was the formation of copper crystals by dewetting the copper films under an Ar–20 %H₂ atmosphere. For this step, the sapphire–copper samples were transferred once again to the sapphire furnace. During experimental runs, the oxygen partial pressure, P(O₂), of the flowing gas was monitored downstream of the sample by means of an external electrochemical oxygen sensor, as described in [16]. After a stable P(O₂) of less than 10^{-21} atm was established, the copper films were

dewetted either in the solid state at 1253 K (TA25) or in the liquid state (TA20 and TA22). The diameter of the resulting copper particles is indicated in Table 1. Samples dewetted in the solid state were annealed at a temperature of 1253 K for 78 h. For dewetting in the liquid state, the temperature was set slightly above the copper melting point (1377 K) for 5 min. The samples were then cooled to 1000 K over a period of 40 min to overcome possible undercooling of the liquid and ensure the solidification of the droplets. Then, the temperature was reset to the annealing temperature of 1253 K for several hours for equilibration of the copper–sapphire interface without excessive evaporation of the copper particles.

The samples were observed by scanning electron microscopy (SEM, Jeol, JSM-6320F). A carbon film was deposited on half of the sample surfaces to avoid charging and facilitate imaging of the copper crystals. On the other half which was left bare, it was possible to image details of the morphology of the sapphire substrate at 3 kV.

The orientation relationships between copper and sapphire were investigated by automated EBSD mapping in a FEI Quanta 200 FE ESEM equipped with an EDAX/TSL orientation system and a Hikari high speed EBSD detector to record the orientations of copper and sapphire. Data were acquired at 30 kV at a sample tilt of 70° with respect to the electron beam. Several carbon-coated areas containing copper particles were scanned in steps of 50 nm, and these were generally merged into a single data set for the purpose of determining the relative frequencies of occurrence of the various ORs. The EBSD data were analyzed with the TSL software to produce pole figures (PFs) and/or inverse pole figures (IPFs).

The samples were also analyzed by X-ray diffraction in a four-circle diffractometer equipped with a copper anode. The angle between the X-rays source and the detector was fixed to the diffraction angle of the (111) planes of copper ($2\theta = 43.29^\circ$). This is close to the diffraction angle of the (11 $\bar{2}$ 3) planes of sapphire which therefore also contribute to the signal. The sample was then analyzed during rotation around an axis perpendicular to the surface (angle ϕ) and around an axis parallel to the surface of the substrate (angle ψ) to obtain pole figures of the (111) and (11 $\bar{2}$ 3) reflections of copper and sapphire, respectively.

Some samples were prepared by focused ion beam (FIB) sectioning for transmission electron microscopy (TEM) observations, in order to check interface flatness at the atomic scale. Data were acquired in a monochromated and aberration corrected field emission gun TEM (FEI Titan 80-300 S/TEM) operated at 300 kV. Kikuchi electron diffraction was used to align the copper particles in a low-index zone axis with surface facets parallel to the viewing direction.

Results

ORs between a-sapphire and Cu particles obtained by dewetting in the liquid state

EBSD results

The orientation relationships of the copper particles dewetted in the liquid state were determined from samples TA20 and TA22 by EBSD. For each sample, the EBSD analysis was performed on data from a few hundred copper particles, taking only one point from each crystal. This procedure assigns the same weight to large and small particles. In the following, the results obtained from sample TA22 are presented. The statistics are based on 748 copper crystals. The data obtained from TA20 are consistent with those of TA22 but are based on fewer (275) crystals.

In Fig. 2, three pole figures of the sapphire substrate allow identification of the crystallographic alignment of the substrate in the microscope reference frame. Figure 2a shows that the a-plane (11 $\bar{2}$ 0) is almost perpendicular to the [001] axis of the microscope stage, and Fig. 2b, c identify the orientations of the two densest directions in the a-plane: [0001] and [1 $\bar{1}$ 00] in the microscope reference frame.

Figure 3 is an inverse pole figure of the copper particles in the [001] direction of the sample reference frame. It shows that copper particles with their (111) planes parallel to the sapphire a-plane occur most frequently. About 38 %

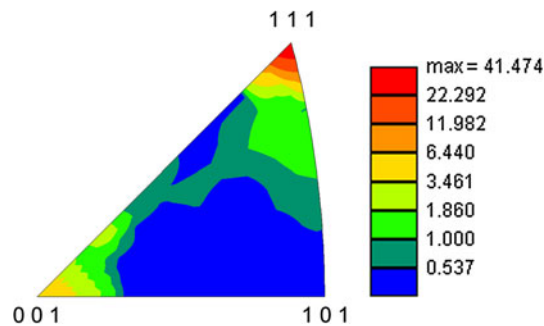
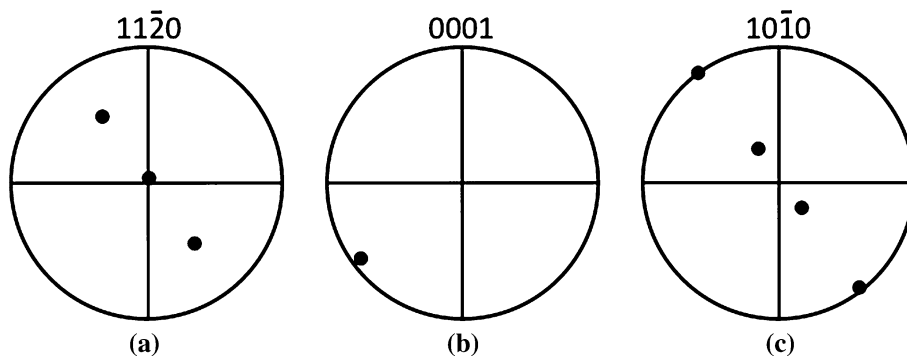


Fig. 3 Inverse pole figure of 748 copper crystals on the a-plane of sapphire after dewetting in the liquid state (sample TA22), in the [001] direction of the sample reference frame. The scale of the color map is in units of multiples of a random distribution (MRD)

of the particles have orientations that fall within 2° of (111). The quantification of the degree of alignment of the (111) plane with the substrate, as given by the TSL-OIM software, is shown in the inset of Fig. 3. It amounts to ~40, in units of multiples of a random distribution (MRD). Crystals of copper with a (100) plane parallel to the substrate are also present, but at much lower frequency (7 % within 2° of (100) or ~6 MRD). In addition, ~55 % of the copper crystals have interface planes that are almost randomly distributed in the stereographic triangle of Fig. 3. A similar analysis of sample TA20, based on a total of 275 crystals, gave 68 % of the copper crystals with (111) interface planes, and 3 % with (100) interface planes. Here, we shall focus primarily on the preferred high frequency OR, namely copper crystals with their (111) planes parallel to the substrate.

In order to determine the full OR of the Cu(111) crystals, additional PFs must be analyzed in comparison with the PF of sapphire of Fig. 2. Figure 4 shows the (110) PF of the copper crystals with their (111) plane parallel to the substrate. The filled circle in the bottom-left quadrant corresponds to the [0001] in-plane direction of sapphire from Fig. 2b. The <110> directions of copper on the edge of the circle do not exactly superimpose on the [0001] in-plane direction of sapphire but are split. They lie within ±3° from the [0001] direction of sapphire. For sample

Fig. 2 Pole figures of three directions of interest in the sapphire substrate TA22, in the microscope reference frame



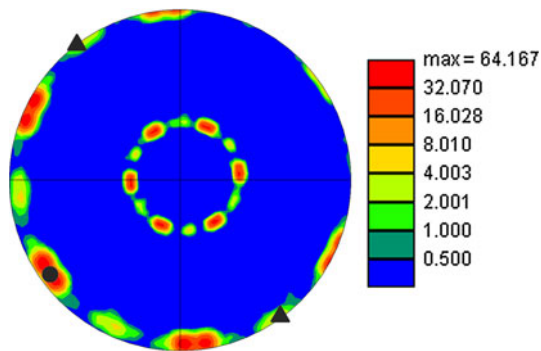


Fig. 4 (110) pole figure of the copper crystals of sample TA22 obtained using only those copper crystals with their (111) planes parallel to the sapphire substrate. The *filled circle* and *triangles* correspond to the [0001] and $[1\bar{1}00]$ poles of the sapphire substrate, respectively. The 110 poles have weak spots corresponding to the sapphire $[1\bar{1}00]$ direction, and two intense spots at $+3^\circ$ and -3° from the sapphire [0001]

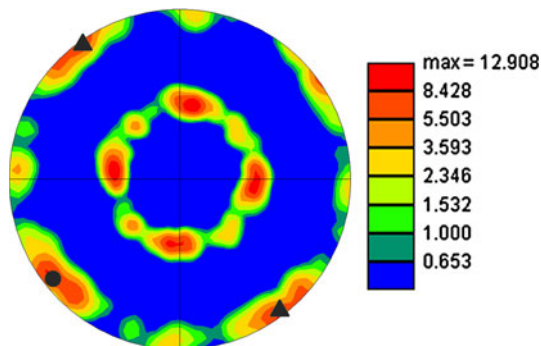


Fig. 5 (110) pole figure of the copper crystals with (001) planes parallel to the sapphire substrate. The *filled circle* and *triangles* correspond to the [0001] and $[1\bar{1}00]$ poles of the sapphire substrate, respectively

TA20, the distance between the two split spots is slightly larger ($\pm 5^\circ$), and the intensity of the spots is not identical. There are additional elongated $(0\bar{1}1)$ spots in the region corresponding to the $[1\bar{1}00]$ direction of sapphire indicated by filled triangles; however, these spots are weaker than the previous ones. From these data, we conclude that there is a preferred OR: $\text{Cu}(111) \parallel \text{Al}_2\text{O}_3(11\bar{2}0)$ with $\text{Cu}[1\bar{1}0]$ within a few degrees of $\text{Al}_2\text{O}_3[0001]$, and a less frequent OR: $\text{Cu}(111) \parallel \text{Al}_2\text{O}_3(11\bar{2}0)$ with $\text{Cu}[1\bar{1}0]$ within a few degrees of $\text{Al}_2\text{O}_3[1\bar{1}00]$.

We also take a brief look at the minority OR composed of copper crystals with their (100) plane parallel to the substrate. Figure 5 shows the (110) PF of those copper crystals. There are four intense split spots occurring every 90° along the edge of the circle. These are superimposed on the [0001] and $[1\bar{1}00]$ in-plane directions of sapphire, indicated by filled circles and triangles, respectively. It is worth noting that the splitting is not symmetric about the

[0001] and $[1\bar{1}00]$ in-plane directions of sapphire but one of the split spots is very close to these two directions.

Since there are two perpendicular sets of close-packed $\langle 110 \rangle$ directions in the (100) copper interface plane, one set is parallel to the $[1\bar{1}00]$ direction of the sapphire a-plane, and the other one is necessarily parallel to the [0001] direction since $[1\bar{1}00]$ and [0001] are perpendicular to each other in the a-plane. Thus, the prevalent OR in this case may be described as follows: $\text{Cu}(100) \parallel \text{Al}_2\text{O}_3(11\bar{2}0)$ with $\text{Cu}[0\bar{1}1]$ within a few degrees from either $\text{Al}_2\text{O}_3[1\bar{1}00]$ or from $\text{Al}_2\text{O}_3[0001]$.

There are also four weaker single spots which occur every 90° (due to the symmetry of (100) planes in fcc lattices) separated from the more intense spots by 40° or 50° . These do not correspond to any low-index direction in the sapphire surface, and have been neglected since they only account for a small fraction of the minority copper crystals with a (100) interface plane orientation.

X-ray diffraction

X-ray diffraction yields information from a large area of the sample surface, and therefore from a larger number of copper crystals than EBSD. Thus, in principle, this approach should yield better statistics than EBSD. Furthermore, it is more precise in defining ORs. However, large crystals contribute more to the XRD signal than small ones, and changes in the orientation relationship due to size effects would not be detected. By EBSD, it is possible to identify and select the particles contributing to the signal whereas by XRD, large polycrystalline particles with grains that are not in contact with the substrate cannot be excluded.

Figure 6a shows the pole figure of the (111) poles of copper together with the $(11\bar{2}3)$ poles of sapphire. From the position of the sapphire poles, it is possible to define the directions of sapphire in the reference frame; the red line in the figure shows the [0001] direction. The (111) poles of copper are located in the center of the pole figure and on the circle at $\psi = 70.5^\circ$ from the center; this means that most of the copper particles have their (111) planes parallel to the substrate. From the six double spots at $\psi = 70.5^\circ$, the $[1\bar{1}0]$ directions of Cu can be defined. Two of them, belonging to two different families of (111) copper crystals, are shown in Fig. 6a by dashed blue lines. The main OR is $\text{Cu}(111) \parallel \text{Al}_2\text{O}_3(11\bar{2}0)$ with $\text{Cu}[1\bar{1}0]$ at $\pm 4^\circ$ from the [0001] direction of sapphire. These results substantially confirm those obtained by EBSD. The intensity of the (111) spots can be seen in Fig. 6b taken at constant $\psi = 70.5^\circ$. Interestingly, one of the two spots is 50 % more intense than the other. However, this is not surprising since the

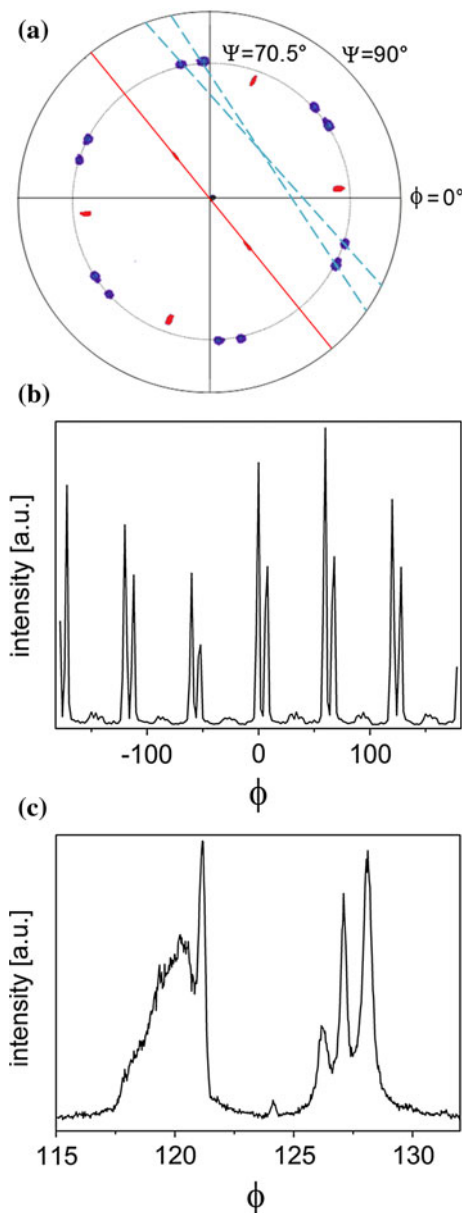


Fig. 6 a Pole figure obtained by X-ray diffraction. Blue and red spots correspond to the (111) poles of copper and the (1123) poles of sapphire (sample T20), respectively. The red line marks the [0001] direction of sapphire, and the blue dashed lines mark the [110] directions of two different families of copper crystals. b Intensity of the (111) poles along a circle at $\psi = 70.5^\circ$ (sample TA22), with the origin of ϕ redefined to correspond to a Cu(111) doublet; the left peak of a doublet is 50 % more intense than the right peak. c High precision scan of one of the doublet peaks of b

sapphire(1120) plane does not display mirror symmetry along the [0001] direction, as noted earlier in connection with Fig. 1. Furthermore, a higher precision scan on a single pair of spots (see Fig. 6c) shows that the peaks on either side of perfect alignment with [0001] appear to be composed of either two or three smaller peaks of varying intensity and different width at half maximum. The small

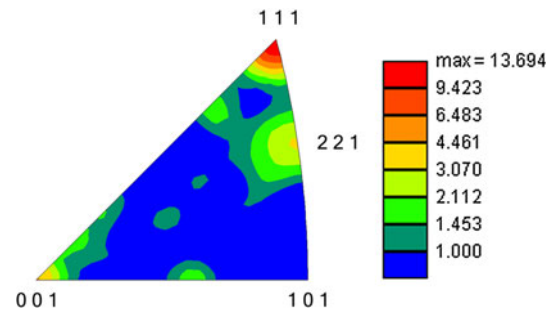


Fig. 7 Inverse pole figure of 253 Cu crystals on the a-plane of sapphire after dewetting in the solid state (sample TA25), in the [001] direction of the sample reference frame

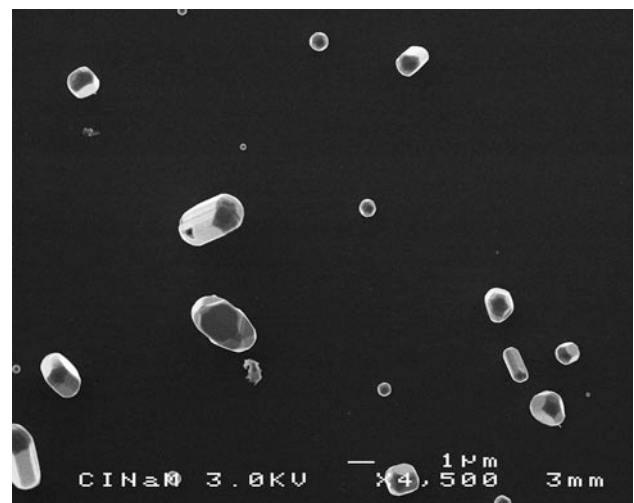


Fig. 8 Image of copper particles from sample TA25 showing the presence of large polycrystalline particles, many of which adopt a rod-like shape

peak at $\phi = 124^\circ$ shows that there are also some crystals with the [110] direction aligned exactly along the [0001] direction of sapphire but they are rare.

OR of Cu on a-sapphire dewetted in the solid state

The orientation relationships of the copper particles dewetted in the solid state were determined by EBSD from sample TA25. The statistics on this sample are based on 253 copper crystals.

Figure 7 is an inverse pole figure of the Cu particles in the [001] direction of the sample reference frame. It shows that copper particles with (111) planes parallel to the sapphire a-plane occur most frequently. However, the copper crystals with the (111) plane parallel to the substrate amount to only 9 % of the total, much less than the 38 % of (111)-oriented Cu crystals found in Fig. 3 for samples dewetted in the liquid state. This significant difference is due to the presence of a fairly large fraction of large polycrystalline copper particles in the shape of short rods

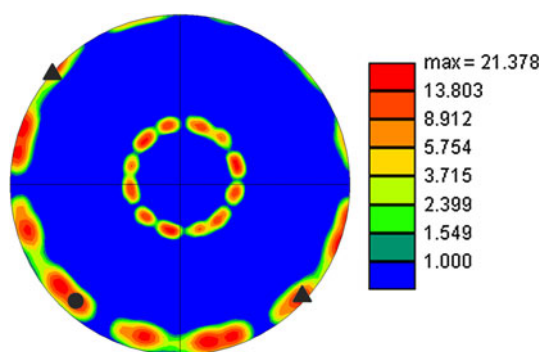


Fig. 9 (110) pole figure of the 35 Cu(111) crystals from a set of 62 crystals from sample TA25; the *filled circle* and *triangles* correspond to the [0001] and $[1\bar{1}00]$ poles of the sapphire substrate, respectively

(see Fig. 8) in the solid state dewetted sample. As in the case of the liquid state dewetted sample, the solid state dewetted samples also contain a smaller fraction of copper particles oriented with their (100) planes parallel to the substrate. In addition, particles with a (221) interface plane occur at a comparable frequency to the (100)-oriented particles. While the (221) interface orientation also appears in samples dewetted in the liquid state at a frequency higher than background (see Fig. 3), the fraction of particles with this orientation in the present case is relatively much larger than that seen after liquid state dewetting.

In order to illustrate the complete OR for solid state dewetting, we use a data set selected from a region of the sample which had a smaller fraction of polycrystalline particles so as to highlight the highest frequency OR. Figure 9 shows the (110) PF of the copper crystals with the (111) plane parallel to the substrate, taken from a data set of 62 copper crystals. In this set, 35 crystals (i.e., 56 %) had their (111) planes parallel to the substrate, and 14 (i.e., 23 %) had their (100) planes aligned with the substrate. The figure also shows the corresponding [0001] and $[1\bar{1}00]$ poles of the sapphire substrate as a filled circle and filled triangles symbols, respectively.

As in the case of the liquid state dewetted samples, the $[1\bar{1}0]$ directions of copper on the edge of the circle are not exactly superimposed on the [0001] pole of sapphire but are split into two spots that lie asymmetrically within 8° of the [0001] pole. There are also additional elongated $(1\bar{1}0)$ spots in the region corresponding to the $[1\bar{1}00]$ direction of sapphire. Thus, we conclude that the preferred OR that develops during solid state dewetting tends toward that obtained after liquid state dewetting, namely: Cu(111) \parallel $\text{Al}_2\text{O}_3(11\bar{2}0)$ and Cu $[1\bar{1}0]$ within a few degrees of $\text{Al}_2\text{O}_3[0001]$, or Cu $[1\bar{1}0]$ within a few degrees of $\text{Al}_2\text{O}_3[1\bar{1}00]$.

X-ray diffraction performed on this sample gives results that are generally similar to those obtained from samples

dewetted in the liquid state, with the exception that the frequency of copper crystals with (221) planes parallel to the substrate is higher than that inferred from the EBSD results. We shall return to these differences in the discussion section.

Triple line, ridges and interface shape

As a copper particle equilibrates with sapphire, the substrate can undergo shape changes that lead to the formation of depressions beneath the particle and the build-up of ridges at the triple line, as described in more detail in the discussion. These changes have been studied here by performing SEM and AFM studies on the bare surface of the samples where some of the smaller copper crystals had evaporated. In addition, the stability of the sapphire a-plane at the copper/sapphire interface has been investigated by TEM on FIB cross-sections through particles and the associated substrate.

Figure 10 shows an SEM image of an uncoated surface of sample TA25, which displays a group of polygonal features related to the ridge, and to the outline of the Cu/ $\alpha\text{-Al}_2\text{O}_3$ interface that is revealed by the evaporation of some of the smaller copper crystals. Both the ridges that have grown at the triple line and the shallow depression beneath the evaporated crystal consist of several facets. The depression often contains a residual nano-crystal of copper. Using images from several regions of the sample, and from the known position of the sample in the SEM stage, it was possible to identify the crystallographic directions in the sapphire crystal, which correspond to the two main traces along the edges of ridge facets; these lie along the $[1\bar{1}00]$ direction and a second unknown direction

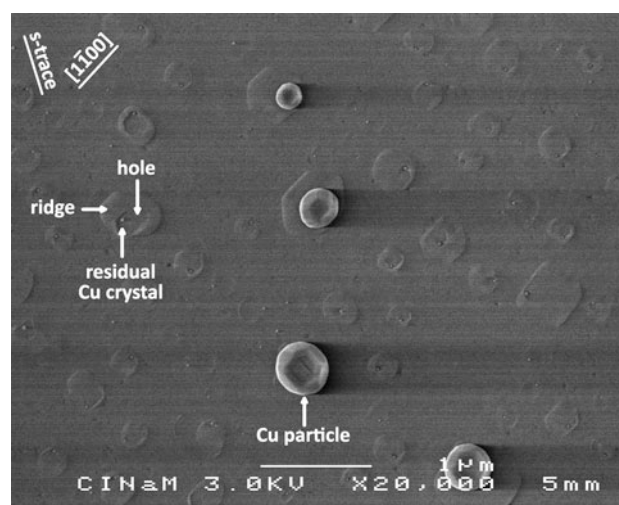


Fig. 10 Secondary electron image of the surface of TA25 showing ridges and changes of shape of the interface between copper crystals and the sapphire substrate after evaporation of copper crystals

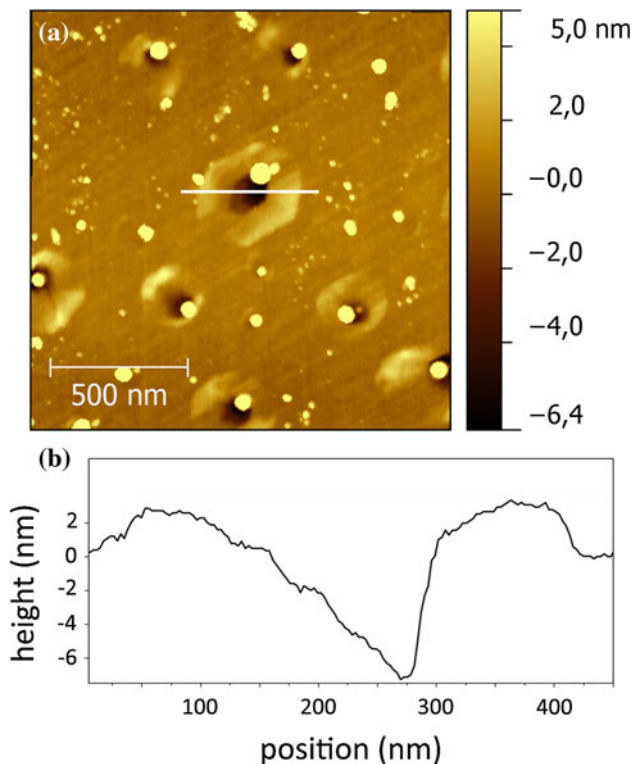


Fig. 11 **a** AFM image of TA25. Bright dots correspond to copper crystals whose size decreased because of copper evaporation during annealing. The cavities remaining after evaporation of the copper crystals have faceted ridges. **b** Profile across a hole taken along the horizontal white line shown in **a**

at about 58° from $[1\bar{1}00]$. The unknown trace could belong to the s-plane ($10\bar{1}1$), which is one of the rhombohedral facets that has been found to be present on the equilibrium crystal shape of sapphire [17, 18] as well as at the interface between sapphire and Pt [19].

Atomic force microscopy was used to measure the dimensions of the ridges and the depth of the cavity beneath the evaporated copper crystals on the sample annealed for the longest duration (TA25). Figure 11a shows the redistribution of alumina that has taken place beneath each copper crystal. In principle, the copper particle must sink into the substrate to reach its equilibrium shape, and the sapphire removed from beneath the particle must be redeposited at the triple line in the shape of ridges. However, as evaporation proceeds, the copper particle size diminishes causing the triple line to recede (although it might be pinned at some points). At this new position, the particle must sink further, eventually leading to a complex profile such as that shown in Fig. 11b. The profile shape depends on the initial position of the triple line, the size of the copper crystal, the period of time over which it evaporated, as well as the directions in which the triple line receded during the evaporation process since the triple line is the location where the ridge is formed. Although ridge

height and depression depth vary in size depending on some of these factors, we estimate the vertical dimensions of these features, after 78 h of annealing, to be of the order of a few tens of nanometers for crystals having an initial size of $1\ \mu\text{m}$ or less.

The profile through an interfacial feature (ridge and depression), displayed in Fig. 11b, shows that the hole is faceted. After complete or partial evaporation of a copper particle, it is not clear whether the bottom of the cavity is parallel to the substrate orientation. However, confirmation of the fact that the bottom of the cavity remains parallel to the substrate has been obtained by sectioning some particles, as described below.

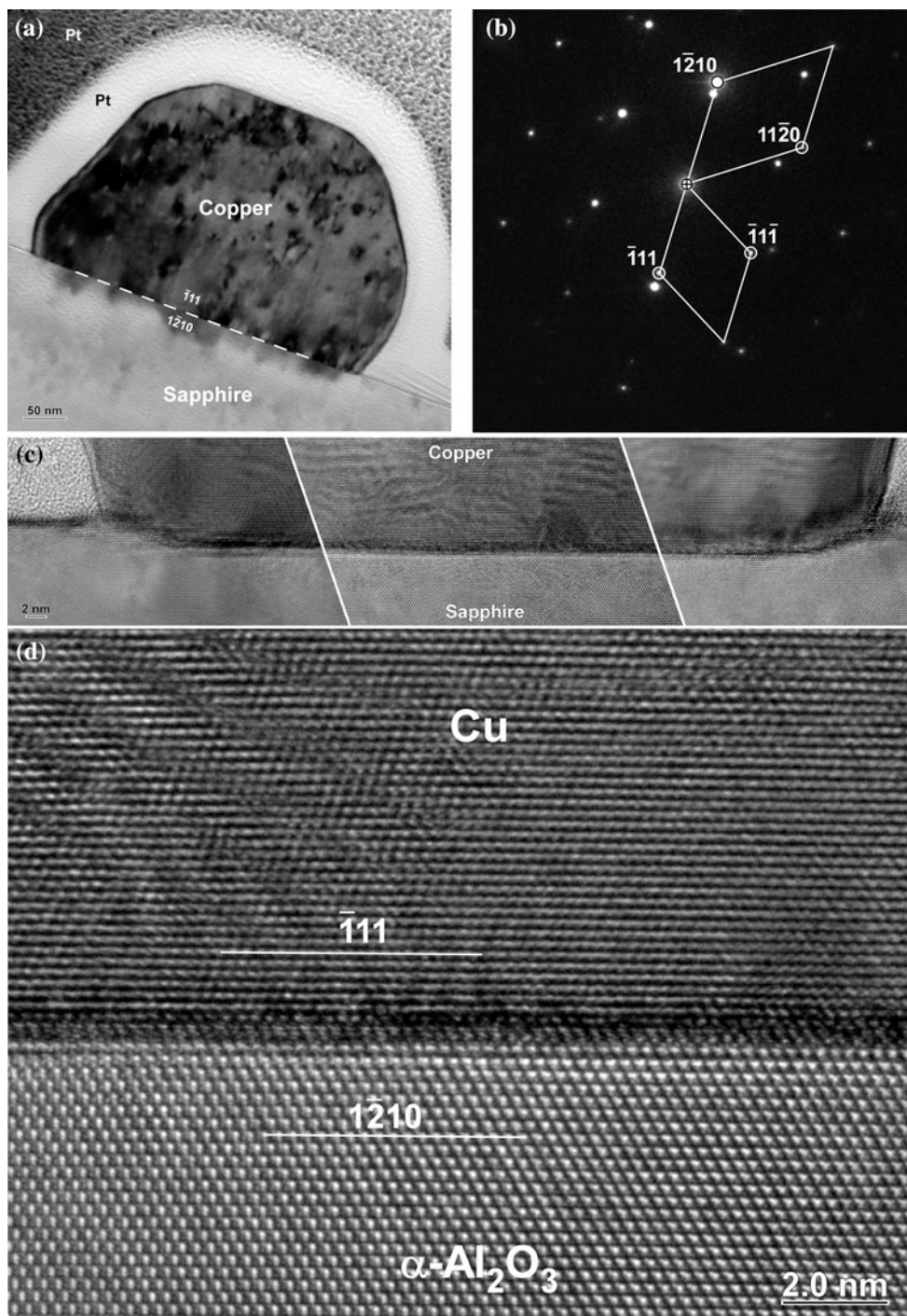
It has been shown previously that the m-plane of sapphire in equilibrium with gold crystals is not stable, and tends to microfacet [20] at a nanometer scale. Although the a-plane is stable on the sapphire equilibrium crystal shape, we have checked whether this plane is stable in contact with copper, i.e. at the Cu/a- Al_2O_3 interface. This has been accomplished by acquiring high resolution TEM images of the interface on samples prepared by cross-sectioning a copper crystal using a dual beam FIB, as previously described for gold particles supported on sapphire [21, 22]. Two copper particles, both displaying $\text{Cu}(111) \parallel \text{Al}_2\text{O}_3(11\bar{2}0)$ but with different alignment of in-plane directions with sapphire, have been investigated. As an example, Fig. 12 shows a copper crystal with $\text{Cu}[1\bar{1}0] \parallel \text{Al}_2\text{O}_3[0001]$ which has sunk into the substrate. The high resolution images (Fig. 12c, d) show that the interface remains atomically flat, thereby confirming the stability of a-plane sapphire at the Cu/sapphire interface.

Discussion

OR of Cu on a-sapphire

The preferred OR identified here for copper particles on a-plane sapphire is $\text{Cu}(111) \parallel \text{Al}_2\text{O}_3(11\bar{2}0)$ and $\text{Cu}[1\bar{1}0] \parallel \text{Al}_2\text{O}_3[0001]$, within few degrees from $\text{Al}_2\text{O}_3[0001]$, whether copper is dewetted in the liquid or the solid state. The most interesting difference between the present observations on a-plane sapphire and the results observed previously for the ORs of copper crystals grown on c-plane sapphire is the prevalent misalignment of the in-plane copper close packed directions with the dense directions that lie in the sapphire interface plane. This misalignment violates the Fecht and Gleiter [3] lock-in model which has invoked (qualitative) arguments to suggest that densely packed directions lying in the metal side of the interface should lie parallel to densely packed directions in the terminating plane on the oxide side of the interface. Several different ORs were

Fig. 12 **a** Bright field TEM micrograph from a FIB cross-section of a copper particle on a-plane sapphire obtained by solid state dewetting. The micrograph was recorded after aligning the sapphire substrate in the [0001] zone axis using Kikuchi electron diffraction. The platinum (Pt) was deposited in the FIB to protect the particle during the subsequent ion milling process. **b** Selected area electron diffraction from the copper particle and sapphire substrate showing the OR. **c** A montage of three high resolution TEM micrographs showing that the Cu(111)/Al₂O₃(11 $\bar{2}$ 0) interface remains atomically flat at the center of the particle and the formation of ridges along the triple lines. **d** A magnified micrograph of the center region of the atomistically flat interface



found for copper crystals on c-plane sapphire [1], namely: Cu(111)[1 $\bar{1}$ 0] \parallel Al₂O₃(0001)[1 $\bar{1}$ 00] for solid state dewetting, and four additional ORs for liquid state dewetting: Cu(111)[1 $\bar{1}$ 0] \parallel Al₂O₃(0001)[11 $\bar{2}$ 0], Cu(110)[1 $\bar{1}$ 0] \parallel Al₂O₃(0001)[11 $\bar{2}$ 0], Cu(311)[01 $\bar{1}$] \parallel Al₂O₃(0001)[11 $\bar{2}$ 0] and Cu(210)[001] \parallel Al₂O₃(0001)[11 $\bar{2}$ 0]. In all these cases, a densely packed direction in the copper interface plane (of type $\langle 110 \rangle$ or $\langle 100 \rangle$) was parallel to one of the two

densely packed directions in the sapphire c-plane ([1 $\bar{1}$ 00] or [11 $\bar{2}$ 0]).

To test whether the misalignment of the copper closed packed directions with the densely packed directions in the sapphire a-plane could be due to improved atomic coincidence across the Cu/a-Al₂O₃ interface at small misalignments, the number of coincidences was computed as a function of small misalignment angles. The results are shown in Fig. 13.

The figure was constructed by using the lattice constants of copper and sapphire corresponding to 1273 K ($a_{\text{Cu}} = 375$ pm [23], $a_{\text{sapphire}} = 480$ pm, $c_{\text{sapphire}} = 1312$ pm [24]), i.e., the room-temperature lattice constants were corrected by the thermal expansion coefficients of both crystals. Coincidences were obtained by considering the a-sapphire surface to consist of one plane of Al ions and two O ion planes closest to the surface. Since exact coincidences between arbitrary lattices cannot generally occur, a tolerance of 25 pm was allowed between the positions of Cu and of the Al and O ions of the sapphire surface (all projected onto the interface plane). Coincidences were counted over an area of a-sapphire of ~ 6500 pm \times 5000 pm. The result shown in the figure was smoothed by means of a five-point averaging scheme in order to remove noise.

Figure 13 shows a number of interesting features. There is a significant and rapid variation in the number of coincidences with small changes in the angle between densely packed rows so that successive maxima and minima can occur over angular changes of the order of a degree. However, the details of the results do depend on the assumed tolerance, as well as on the particular point at which the copper and sapphire planes are matched (see Fig. 13). Nevertheless, the results shown in the figure provide a suggestive qualitative match to the X-ray

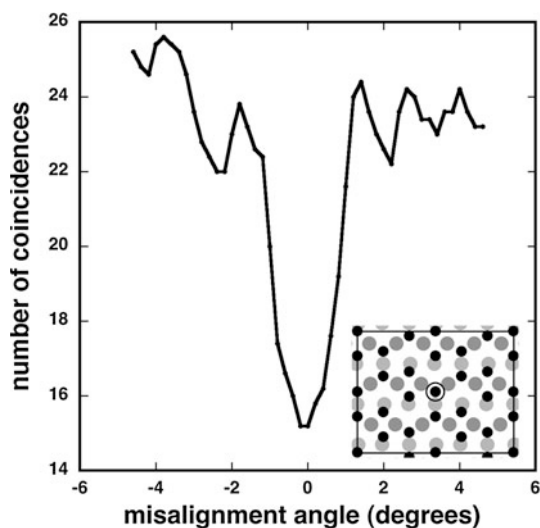


Fig. 13 Calculated coincidences between the atoms of copper(111) with the ions of the (11 $\bar{2}$ 0) sapphire plane, as a function of misalignment angle between Cu[110] and sapphire[0001] (see text). The inset shows a unit cell of the sapphire a-plane surface indicating the positions of Al ions (small black circles) and the first two planes of O ions (larger dark gray and light gray circles); the circled Al ion shows the particular point which was chosen as the site of perfect coincidence with Cu for the calculations. The details of the results depend on the particular point at which the copper and sapphire planes are matched

intensity as a function of misorientation displayed earlier in Fig. 6c.

Thus, we suggest that the misalignment of the Cu $\langle 110 \rangle$ directions with the densely packed sapphire direction [0001] in the ORs observed here on the a-plane is most likely due to the high coincidence between copper atoms and all of the sapphire sites at the interface plane, which outweighs alignment of the densely packed directions. It should be emphasized that Fig. 13 was constructed based on the assumption of an ideal interface without allowing for any atomic relaxation or possible interfacial reconstruction. More details on the interface structure at the atomic level would require an extensive investigation by HRTEM.

Certain differences have been observed between samples prepared by dewetting of copper in the solid versus the liquid state. After solid state dewetting, there is a significant fraction of large polycrystalline copper particles, many of which adopt a rod-like shape. These rod-shaped particles are not seen in liquid state dewetted samples. In addition, while the frequency of (111)-oriented copper crystals was smaller in the case of solid state dewetted samples, the frequency of (221) oriented crystals was significantly larger than in samples dewetted in the liquid state. Copper crystals, which display a [221] direction normal to the substrate, can develop in particles which possess a (100) interface with the substrate but which also contain twin boundaries. Since there are more polycrystalline particles in the solid state dewetted sample, we suspect that the higher fraction of (221) oriented crystals arise by twinning of particles with (100) interfaces.

Morphology of the interface

As mentioned in the introduction, when a particle partially wets a flat substrate, the vertical forces due to the various surface energies acting at the triple line are unbalanced. An anisotropic faceted crystal in equilibrium on a substrate can adopt various configurations, as calculated by Siem et al. [13]. Figure 14 is a schematic representation of two possible configurations for such a crystal equilibrated on an initially flat substrate. The configuration shown in Fig. 14a, where the substrate remains flat, will tend to persist if the torques associated with the substrate surface energy and/or the particle/substrate interfacial energy are sufficiently large to balance out the vertical forces [25]. This type of configuration was observed for the case of copper particles on c-plane sapphire [1] and for gold and nickel on c-plane sapphire [21, 26]. Such a configuration may also persist, even in the absence of large substrate torques, in cases where insufficient time is provided during the experiment for the substrate shape at the interface to evolve by diffusive processes. In the event that substrate torques are not

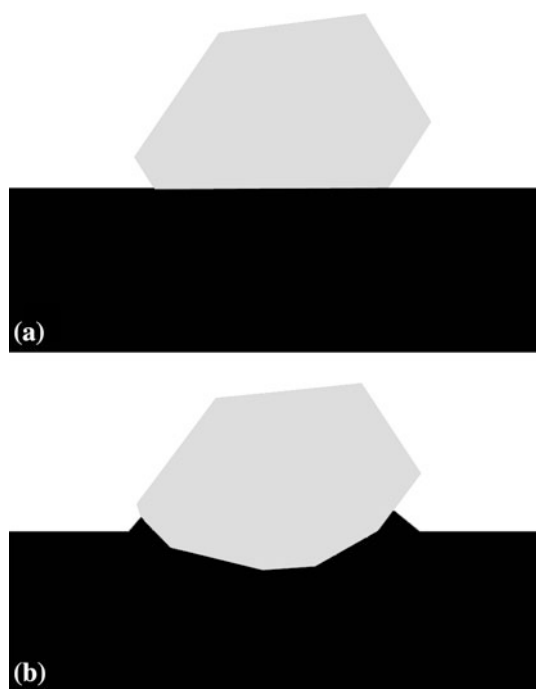


Fig. 14 Schematic configurations of a faceted particle on a substrate, (a) without and (b) with shape equilibration of substrate

large enough to balance the vertical forces due to surface energies and mass transport is sufficiently rapid, matter will be transported to the triple line to form ridges around the particle; this allows a proper local balance of forces to prevail [11, 12, 25]. A possible result is shown schematically in Fig. 14b where two phenomena are displayed: ridge formation around the particle and faceting of the depression which forms beneath the particle when matter is transported to the ridge. In an isotropic case, the ridge would be a transient feature that eventually disappears by spreading onto the substrate surface. However, for anisotropic interfacial energies, it is also possible for ridges to be an integral part of the shape of a crystal in equilibrium with a substrate due to the additional puckering of the substrate interface that may be needed to accommodate the junction with the particle surface [13].

Figure 15a shows a sketch of the shape of a copper crystal on a sapphire surface when its total energy is minimized under the assumption that all energies are isotropic (the construction of this shape is explained in the caption). The surface and interfacial energies used in Fig. 15a have been taken from the literature (for the copper surface [27], for the sapphire surface [28], for the copper/sapphire interface [1]). The figure shows that under these simplifying assumptions, the distance of the apex of the interfacial cap from the substrate surface is 45 % of the total height of the copper particle above the surface level. The depth of the interface below the sapphire surface and

the height of the ridges that we have observed and measured by AFM are much smaller than those calculated here. Thus, we conclude that the interface has not reached its equilibrium shape by the time the copper crystal has evaporated.

Whereas Fig. 15a provides a rough idea of the relative size of the depression that will form below a copper particle for the case of isotropic interfaces, in the case of anisotropic interfaces the interfacial region could be replaced by a much more complex faceted shape [13, 14]. Figure 15b presents two views of the equilibrium shape calculated by means of the Wulffmaker software [14] for the case of a copper particle on a sapphire substrate where the orientation relationship is $\text{Cu}(111)[\bar{1}\bar{1}0] \parallel \text{sapphire}(11\bar{2}0)[1\bar{1}00]$. In order to produce Fig. 15b, we have assumed the absolute values of surface and interface energies used to calculate Fig. 15a. For clarity, the surface energy anisotropy of copper relative to the (111) plane has been taken to be equal to 1.06 for the (001) plane and 1.07 for the other orientations. Furthermore, we have made two simplifications: in the absence of experimental data, the energy anisotropy of the copper/sapphire interface has been taken to be identical to that of the sapphire surface [17, 18], and the energy of the sapphire surface has been taken to be constant since the current version of the Wulffmaker is unable to account for any effects arising from the anisotropy of the substrate surface. In spite of these simplifications, some interesting results have been obtained.

In Fig. 15b, the thick white line represents the triple line, and the dotted horizontal line indicates the position of the sapphire surface. This triple line does not lie in any given plane, so that the surface of the substrate must pucker in order to minimize total interfacial energy. The upper part of the shape above the triple line represents the copper crystal, where (111) and (100) facets have been colored blue and green, respectively. The rest of the copper surface (gray) should appear rounded, but is faceted because Wulffmaker can only handle a finite number of orientations. The lower part of the shape below the triple line represents the copper-sapphire interface; the orange, purple, and yellow facets correspond to the sapphire $r(\bar{1}\bar{1}02)$, $p(11\bar{2}3)$ and $s(10\bar{1}1)$ planes, respectively. The bottom facet which is parallel to the substrate surface and colored in red in Fig. 16a, is oriented along $(11\bar{2}0)$, or the a-plane. Therefore, a part of the copper-sapphire interface is parallel to the substrate surface.

Figure 16a shows a projection of the triple line onto the substrate as calculated by Wulffmaker, and Fig. 16b shows an SEM micrograph of a triple line on the sapphire substrate, as revealed by a partially evaporated copper crystal. In spite of the approximations of the Wulffmaker calculations, there appears to be a reasonable match between the experimental and calculated triple line shapes.

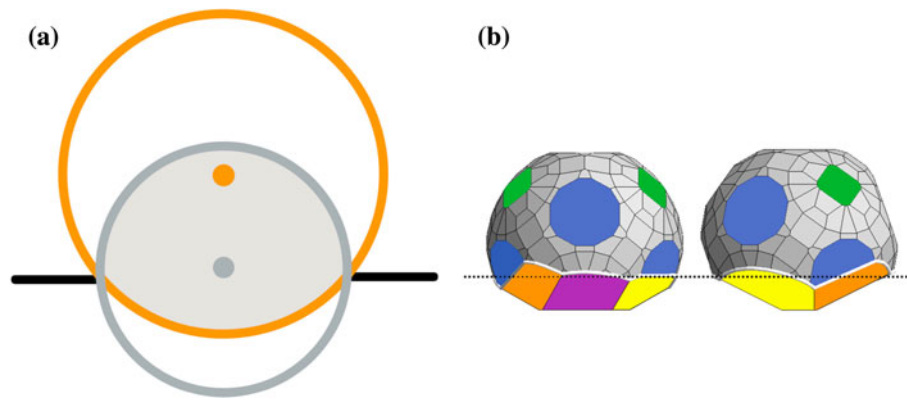
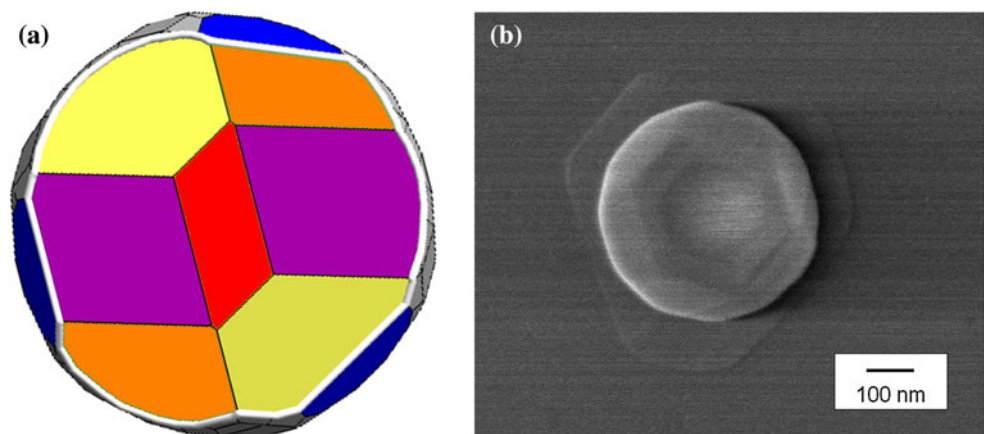


Fig. 15 **a** Isotropic equilibrium shape of a copper particle in contact with a sapphire surface. The two *circles* correspond to the Wulff plots of the copper surface (*gray*) and the copper/sapphire interface (*orange*). Their radii scale with the energy of the copper surface and of the copper/sapphire interface, respectively, and their Wulff centers are displaced by the sapphire surface energy. The sapphire surface (*black line*) is located at the intersections of the *circles*. The copper particle occupies the *light gray* region. **b** Equilibrium crystal shape of a faceted copper particle on an *a*-sapphire substrate calculated with Wulffmaker. The *thick white line* represents the triple line and the

horizontal black dotted line represents the position of the sapphire surface. *Blue* and *green* facets correspond to the $\{111\}$ and $\{100\}$ orientations of copper, respectively. *Orange*, *purple*, and *yellow* facets correspond to the $r\{1\bar{1}02\}$, $p\{11\bar{2}3\}$, $s\{10\bar{1}1\}$ sapphire planes, respectively. The bottom facet parallel to the substrate is the $\{1\bar{1}\bar{2}0\}$ sapphire plane. It can be seen in Fig. 16a where it is colored in red. The energy anisotropy of the interfacial facets relative to the (0001) plane are 1.05, 1.06, 1.07, and 1.12 for the $r\{1\bar{1}02\}$, $p\{11\bar{2}3\}$, $s\{10\bar{1}1\}$ and $a\{11\bar{2}0\}$ planes, respectively

Fig. 16 **a** Shape of the interface and of the triple line of a copper particle on an *a*-sapphire seen from below, through the sapphire substrate, as calculated by means of Wulffmaker. See caption of Fig. 15b for facet planes and colors. **b** SEM photomicrograph of a triple line shape, as revealed on the sapphire substrate by partial evaporation of the copper particle



One last point needs to be addressed. The change of shape of the interface from flat to faceted is energetically driven, and the ridges are part of the equilibrium shape of the interface. The formation of the depression beneath a particle, and the associated ridge, cannot be due to the dissolution of Al_2O_3 in the particle at the annealing temperature, and its reprecipitation around the particle upon cooling, because the solubility of Al_2O_3 in Cu is too low [12, 29] to account for the relatively deep depressions we have observed. If dissolution–reprecipitation were the mechanisms leading to the formation of depressions and ridges, these features should also have been found at the interface between copper particles and (0001) sapphire, which is not the case [1]. We conclude that the mechanism leading to the observed morphology of the interface is diffusion of Al_2O_3 , either along the copper/sapphire

interface or through the copper particle at the annealing temperature, and that it is driven by an attempt of the system to reach the type of equilibrium shape suggested by the calculations performed here with the Wulffmaker software.

Summary and conclusions

1. The dominant OR between copper particles and the *a*-sapphire substrate equilibrated by liquid state dewetting is $\text{Cu}(111) \parallel \text{Al}_2\text{O}_3(11\bar{2}0)$ and $\text{Cu}[1\bar{1}0]$ within few degrees from $\text{Al}_2\text{O}_3[0001]$. A secondary, lower frequency OR is also observed: $\text{Cu}(001) \parallel \text{Al}_2\text{O}_3(11\bar{2}0)$ with $\text{Cu}[1\bar{1}0]$ within a few degrees from either $\text{Al}_2\text{O}_3[1\bar{1}00]$ or from $\text{Al}_2\text{O}_3[0001]$.

2. The dominant OR for samples equilibrated in the solid state is the same, although it appears at a lower frequency. In addition, the increased presence of rod-shaped and other polycrystalline copper particles produce a relatively high frequency of crystals with [221] directions perpendicular to the substrate, which are presumed to arise as twins of copper crystals with (001) planes parallel to the substrate.
3. All ORs show deviations from alignment of the copper close-packed direction with densely packed substrate directions. Thus, the present results do not follow the expectations of the Fecht and Gleiter model which predicts alignment of dense directions in the metal and in the oxide across the interface. An analysis of coincidence across the interface indicates that misalignments are most likely due to improved coincidence at small deviations from ideal alignment.
4. High resolution TEM of the copper (111)/a-sapphire interface shows that the sapphire a-plane remains stable (does not micro-facet). This indicates that the sapphire a-plane is part of the equilibrium shape of the copper/sapphire interface.
5. The initially flat a-sapphire substrate undergoes significant shape changes during equilibration with copper particles. The copper particles sink into the substrate by transport of sapphire from the region beneath the particle to ridges that develop at the triple line. An analysis of the results by means of the Wulffmaker software suggests that these features result from an attempt of the system to reach its equilibrium shape.

Acknowledgements This document has been produced with the partial financial assistance of the European Union as part of the MACAN project as part of the Seventh Framework Programme (2007–2013) under grant agreement FP7-NMP-2009-CSA-233484. The authors thank Rachel Zucker for her assistance in using the Wulffmaker software. SC, DC, HM, and WDK acknowledge partial support from the Ministry of Science and Technology, Israel, and the Ministry of Research, France. HM and WDK acknowledge support from the Russell Berrie Institute for Nanotechnology at the Technion. GSR acknowledges support from the Office of Naval Research Grant

N00014-11-1-0678. Lastly, HC and PW acknowledge support of their research by the MRSEC Program of the National Science Foundation under Award No. DMR-0520425. Facilities support from the Carnegie Mellon MRSEC, under National Science Foundation Award Number DMR-0520425, are also acknowledged.

References

1. Curiotto S, Chien H, Meltzmann H, Wynblatt P, Roher GS, Kaplan WD, Chatain D (2011) *Acta Mater* 59:5320
2. Chatain D, Ghetta V, Wynblatt P (2004) *Interface Sci* 12:7
3. Fecht H, Gleiter H (1985) *Acta Metall* 33(4):557
4. Sasaki T, Matsunaga K, Ohta H, Hosono H, Yamamoto T, Ikuhara Y (2003) *Sci Technol Adv Mater* 4:575
5. Herrmann G, Gleiter H (1976) *Acta Metall Mater* 24(4):353
6. Oh SH, Scheu C, Wagner T, Ruhle M (2007) *Appl Phys Lett* 91:141912
7. Scheu C, Stein W, Ruhle M (2000) *Phys Status Solid B* 222:199
8. Vargas R, Goto T, Zhang W, Hirai T (1994) *Appl Phys Lett* 65:1094
9. Dai Z, Bednarski-Meinke C, Loloee R, Golding B (2003) *Appl Phys Lett* 82:3847
10. Liu Y, German RM (1996) *Acta Mater* 44:1657
11. Saiz E, Tomsia AP, Cannon RM (1998) *Acta Mater* 46:2349
12. Ghetta V, Chatain D (2002) *J Am Ceram Soc* 85(4):961
13. Siem EJ, Carter WC, Chatain D (2004) *Philos Mag* 84(10):991
14. Zucker RV, Chatain D, Dahmen U, Hagege S, Carter WC (2012) *J Mater Sci* 47:8290
15. Curiotto S, Chatain D (2009) *Surf Sci* 603:2688
16. Chatain D, Chabert F, Ghetta V, Fouletier J (1993) *J Am Ceram Soc* 76:1568
17. Choi J-H, Kim D-Y, Hockey BJ, Wiederhorn SM, Handwerker CA, Blendell JE, Carter WC, Roosen AR (1997) *J Am Ceram Soc* 80:62
18. Kitayama M, Glaeser AM (2002) *J Am Ceram Soc* 85:611
19. Santala MK, Radmilovic V, Giulian R, Ridgway MC, Gronsky R, Glaeser AM (2011) *Acta Mater* 59(12):4761
20. Sadan H, Kaplan WD (2006) *J Mater Sci* 41:5371
21. Sadan H, Kaplan WD (2006) *J Mater Sci* 41:5099
22. Baram M, Kaplan WD (2008) *J Microsc* 232:395
23. Bennet S (1978) *J Phys D Appl Phys* 11:777
24. Aldebert P, Traverse JP (1982) *J Am Ceram Soc* 65:460
25. Chatain D, Carter WC (2004) *Nat Mater* 13(12):843
26. Meltzman H, Mordehai D, Kaplan WD (2012) *Acta Mater* 60(11):4359
27. Kumikov VM, Khokonov KB (1983) *J Appl Phys* 54:1346
28. Levi G, Kaplan WD (2003) *Acta Mater* 51:2793
29. Trumble KP (1992) *Acta Metall Mater* 40:s105